The Chemical Record 18 (2018): 1065-1075

DOI: http://doi.org/10.1002/tcr.201700094

Investigating the potential barrier function of nanostructured materials formed in engineered barrier systems (EBS) designed for nuclear waste isolation

Jaime Cuevas*, Ana Isabel Ruiz and Raúl Fernández

Department of Geology and Geochemistry, Faculty of Sciences, Autonomous University of Madrid, C/ Tomás y Valiente 7, 28049 Madrid, Spain. E-mail: Jaime.cuevas@uam.es

Abstract

Clay and cement are known nano-colloids originating from natural processes or traditional materials technology. Currently, they are used together as part of the engineered barrier system (EBS) to isolate high-level nuclear waste (HLW) metallic containers in deep geological repositories (DGR). The EBS should prevent radionuclide (RN) migration into the biosphere until the canisters fail, which is not expected for approximately 10^3 years. The interactions of cementitious materials with bentonite swelling clay have been the scope of our research team at the Autonomous University of Madrid (UAM) with participation in several European Union (EU) projects from 1998 up to now. Here, we describe the mineral and chemical nature and microstructure of the alteration rim generated by the contact between concrete and bentonite. Its ability to buffer the surrounding chemical environment may have potential for further protection against RN migration.

Keywords

Clay, cement, nanocolloid, nuclear waste isolation, geochemical buffer

Introduction

Clay and cement are known nano-colloids originating from natural processes or traditional materials technology [1]. Their final chemical and structural forms are created by hydration or aqueous dissolution-precipitation reactions, which affect anhydrous primary minerals[2] and weathering, even on the surface of Mars [3], or the hydration of synthetic phases produced in the calcination of geomaterials[4]. A common feature in these materials is that they are composed of hydrated nanophases, and with metal oxides, they develop (cement[5]) rims around primary materials. These rims should act as metastable physico-chemical barriers to prevent a rapid alteration process[6].

Our research group at the Autonomous University of Madrid (UAM) has participated in several UE integrated projects under the Euratom Framework Programme for Nuclear Research & Training Activities (ECOCLAY-I and II 1998-2003)[7], NFpro (2004-2007) and PEBS (2010-2014)[8]. In these projects, we studied the alkaline alteration that characterizes the geochemical reactions in concrete and bentonite materials used for nuclear waste isolation. Bentonite is composed of

smectite sheet-silicate organized as aggregates of stacked layers. These aggregates swell driven by the hydration of the cations confined in their nanostructured interlayers. These interlayers can accommodate water and many ionic and polar pollutant substances[9, 10]. After the 18th year, the FEBEX[11] (full-scale engineered barriers experiment) in situ experiment was dismantled in 2015. We are determining the long-term reactivity of concrete-bentonite interfaces during the development of the CEBAMA (cement-based materials) UE project[12]. In this paper, we describe the structure of these interfaces and show that the developed alteration rim produced has a limited extension and may be a new skin worth studying due to its potential protective capacity.

Review topics and prospect

Radioactive waste and trusted materials for underground high-level waste repository safety

A deep geological repository (DGR) is currently accepted as the most reliable final management option for the long-term isolation of high-level radioactive waste (HLW)[13]. The heat released by HLW due to Cs, Sr and Co radioisotope decay may last for 10^2-10^3 years, and the radiotoxicity of waste due to long-lived transuranic elements such as Am, Pu, and Tc will remain above safety standards for up to 10^4 to 10^6 years [14]. All DRG concepts call for the use of a multi-barrier system (engineered barrier system, EBS) to fulfill the safety requirements to limit the eventual release of radionuclides into the biosphere. The EBS usually has three main components: the waste form, the metal waste canister and the clay buffer. Liners such as metal meshes or concrete sleeves and mechanical supports such as compacted bentonite blocks may be added to the basic design (Figure 1). Using a stiff clay host rock as an example, concrete should be installed as a supporting annulus for the galleries and for the placement of plugs for close galleries containing several aligned waste canisters.

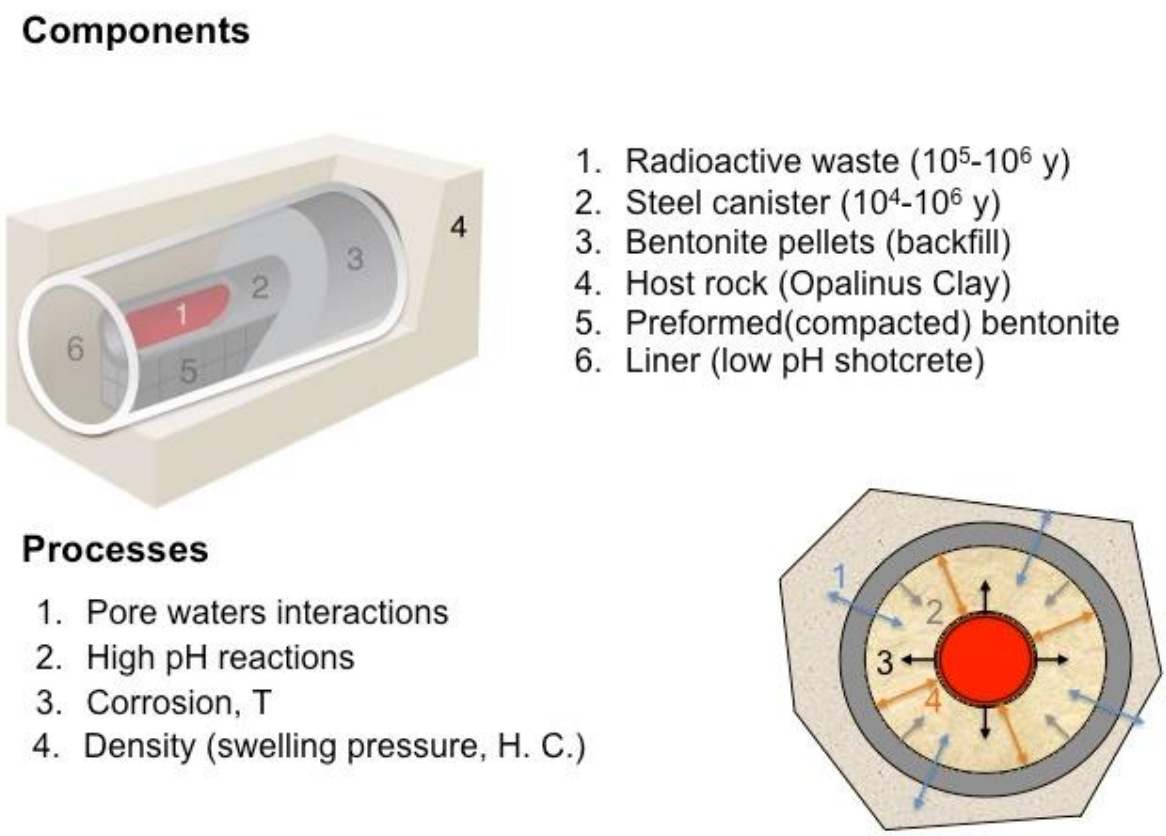

Figure 1. Components of the near-field for a HLW repository system. Process development at the interfaces (modified from Nagra)[15].

Both concrete and metallic canisters (iron steel) are artificial barriers composed of chemical constituents that are far from the aqueous solution thermochemical equilibrium in a groundwater geological environment. Iron steel is known to experience a very slow anoxic corrosion rate in terms of less than 1 µm/year, and its failure is not expected until > 10^3 years[16]. Concrete aging and degradation are not easy to measure. A consecutive set of chemical reactions are produced by groundwater (pH 8-9 in clay or granite host rocks) interactions with concrete porewater originating from ordinary Portland cement (OPC), (pH > 13). The pH during the concrete aging will first be controlled by alkali hydroxides, then by the dissolution of portlandite [$Ca(OH)_2$], pH 12.6, and later, between the pH values of 12.6 and 10, by the dissolution of calcium from C–S–H (calcium silicate hydrate), generating different gel phases and dissolution-precipitation processes with Ca/Si ratios from 1.6 to 0.6[17]. During these stages, the reactions may coexist with the precipitation of $Mg(OH)_2$ (brucite) and $CaCO_3$ (calcite) because Ca, Mg and inorganic carbon species are present in a natural aqueous environment. The precipitation of several hydrated minerals in the concrete matrix will reduce the porosity and reaction-transport processes, and a pessimistic estimation of the partial alteration is 20 cm in 10^5 years[18]. A similar thickness of bentonite will be affected by the reaction of the concrete alkaline plume within the same timeframe. Nevertheless, experiments carried out to study the equilibrium conditions with montmorillonite (smectite) and portlandite have shown consistency with low Ca/Si (0.8) C-S-H (11 Å, tobermorite), which is in agreement with the existence of a montmorillonite-CSH thermochemical equilibrium[19]. The achievement of such conditions should

stop or maintain a very slow rate of reaction for both bentonite and concrete degradation in these EBS contacts. Taking into account that bentonite is a natural alteration product of volcanic glass known to be stable for > 10^6 years[20], the EBS system is a reasonable engineered architecture to ensure the safety of the design through continuous long-term modeling validation of the geochemical and hydro-mechanical performances of the system.

In the nuclear field, concrete is not solely used as a construction material. Hydrated cementitious nanophases such as C-S-H or Afm (Ca, Al, monosulfate) retain oxyanion species of radionuclides, such as Se, U, or Np, by sorption, surface complexation and co-precipitation mechanisms [17, 21]. Porewaters from either bentonite or the host rock in contact with the composites of cement and radioactive waste will be buffered by the formation and dissolution of calcium silicate hydrates. Hence, a multifunctional barrier can be expected in these complex, artificial-natural interfaces.

Interaction of concrete with clay rocks or buffer materials: from lab-scale to full-scale experiments

In the present paper, the results from three experimental setups were considered. The experiments exhibit conditions with different complexities, including reaction mixtures in batch reactors[22, 23], long-term concrete–bentonite column experiments (10 years)[23, 24], and results from the concrete-bentonite in situ FEBEX experiment (13-year-old interface)[25, 26]. Three testing scenarios composed the framework of the research. The in situ concrete-bentonite interfaces, which were obtained during the dismantling of the FEBEX tunnel at the Grimsel test site (GTS) (Switzerland), represent an aged interface within a 50 m^3 experiment (10 m^3 concrete plug and 40 m^3 heated bentonite) hosted in a granitic rock. HB6 is part of a series of HB tests (1-5 are already dismantled) implemented by CIEMAT (Centro de Investigaciones Energéticas, Ambientales y Tecnológicas, SPAIN) and consists of a bentonite cylinder column (7 cm length) hydrated through a high pH OPC concrete disc (3 cm). On the opposite side, the bentonite faces a hot steel plate maintained at 100 °C. HB6 represents a 385 cm^3 10-year-old experiment (115 cm^3 concrete and 270 cm^3 bentonite). In both cases, the concrete-bentonite interface was < 40 °C. Finally, the batch experiments consisted of creating different mixtures of smectite extracted from bentonite with $Ca(OH)_2$, OPC (CEM-I) cement paste or alkali-treated OPC to precipitate $Mg(OH)_2$ close to the exchange complexes located in the interlayer spaces of the swelling silicate sheets. All these experiments consider the presence of calcite at different temperatures. An exhaustive description of the experimental procedures is published elsewhere and is summarized in Table 1.

The purpose of performing the experiments at different scales was to link the cement paste/clay reactivity to the in situ-scale real experiment. In fact, the difficulties encountered in the chemical and mineralogical characterizations of the scenarios close to the real conditions prompted us to perform batch synthetic experiments. This was necessary to determine the types of phases that are produced and to try to find them in the compacted bentonite-concrete experimental interfaces.

Figure 2: Aspect of the Grimsel Test Site in situ sampling, preparation of the samples and images of the polished sections containing the bentonite-concrete contact. Cylinders at the front of the gallery are resin protected for the practice core drilling performed by the University of Bern.

Table 1: Summary of the experiment types and conditions.

Experiment type	Number of experiments	materials	dimensions	Hydration	T (ºC)	time
In situ FEBEX[26]	1	Concrete CEM-II (CEM-I <10% lime added)	Cylindrical gallery 2.3 x 3 m	Granitic site groundwater diluted (<0.01 M) Na-Ca-Cl-SO4-HCO3; pH 8-9	Concrete bentonite contact at 30 ºC	13 years
		FEBEX bentonite 1.65 g/cm^3 dry density	Cylindrical gallery 2.3 x 9 m			
Medium cells HB (CIEMAT)[24]	5	Concrete CEM-I-SR	Cylindrical 70 × 30 mm	Clayey saline (0.2 M) solution Na^+-SO_4^{2-} dominant	Gradient, 100 ºC at bottom (bentonite) ~40 ºC at the interface	1, 1,5, 4.5 6.5 and 10 years
		FEBEX bentonite 1.65 g/cm^3 dry density	70 × 71.5 mm			
Batch experiments[22, 23], *:unpublished **: three Mnt described in[27]	4	FEBEX bentonite < 2 μm (montmorillonite, Mnt)	Powder 1:5 Solid:aqueous solution, airtight inert reactor	$Ca(OH)_2$ at 2/1 and 3/1 Mnt/ Ca(OH)2 ratio	60, 120 ºC	2 months
	6*	Mnt FEBEX, MX-80 and Mmt-Chile		Mg saturated Mnt 2/1 Mnt /CEM-I paste ratio	60, 90 ºC	1 month
	6*	Mnt FEBEX, MX-80 and Mmt-Chile**		Mg saturated Mnt K,Na (3,1)-OH pH 13.5 20/1 Mnt/calcite	60 ºC	1 week

The nature of the nanostructured materials formed and the concrete-bentonite interface zone

The best image capturing the complexity of the chemical perturbation in one of the studied 13-year-old in situ concrete-bentonite interfaces is a typical SEM-EDX profile of the interface (Figure 3). The profiles depicted for the variations in the weight percent of the major elements show a relevant increase in Mg from 1 mm in the concrete side to 2.5 mm in the bentonite side. With an average variation of ±0.5 and ±2 mm in the concrete and bentonite, respectively, the rim has been measured and studied in at least three HB cells (4.5, 6 and 10 years)[23], four interfaces in the FEBEX in situ experiment[26], two portlandite/bentonite interfaces in small cells (5-mm-thick lime mortar and 2-cm-thick compacted bentonite)[28], and at 60-90 ºC in the alkaline alteration (K,Na-OH, pH=13.5 solution) of a 2-cm-thick Mg-saturated, compacted FEBEX bentonite[29]. Calcite precipitates in concrete when the Mg-enrichment peak ends after a millimetric rim, and a Ca,Si (Al)-rich region develops as the Mg decreases (i.e., a calcium aluminum silicate hydrate phase (C-A-S-H)). An example of the Mg-rich phases at the in situ interface is shown in Figure 4.

The chemistry and structural nature of the formed Mg phase is not easy to determine. From a chemical point of view, Figure 4 show that Al ratio to silica remains very close to that of 2:1 Al-di-octahedral montmorillonite alongside the Mg-rich rim transect. In addition, the rate of the Mg increase is consistent with the mixtures of brucite and montmorillonite. However, there is some evidence of the presence of a Mg-trioctahedral sheet silicates.

These chemical trends were examined by X-ray diffraction powder analyses of very small bentonite samples that were scraped from the concrete interface (Figure 5, Left). The in situ or long-term interfaces (HB6) exhibited large shoulders in the Mnt basal reflection XRD regions. The 14.7 Å Mnt (001) peak corresponding to the hydrated sheet unit of the FEBEX montmorillonite changes to a broad shoulder ranging from 14 to 7.4 Å, and from 14 to 9 Å, tobermorite can have diffraction effects [30, 31]. The step at 7.4 Å, the plateau between 2.56-2.40 and the reflection at 1.53 Å ((060) reflection for serpentine minerals) are consistent with the coexistence of brucite intercalated with montmorillonite (chlorite-like, 7 Å) or serpentine[29]. The (060) region exhibits a broad maximum between the tri-octhedral and di-octahedral (as Mnt) silicate sheets, and thus, tri-octahedral 2:1 silicate sheets cannot be excluded. In any case, the patterns are indicative of the formation of disordered minerals with very similar aspects to the magnesium silicate hydrates described to precipitate in cement-clay interactions[32]. The interaction between Mnt and the cement paste or lime confirms the possible formation of poorly ordered phases in the range of 14 to 11 Å and contributes to the complex mixture of these sheet-like structures (Figure 5, right). Al-tobermorite (C-A-S-H) formed, and the presence of calcite makes it difficult to determine its presence. In any case, these results are in agreement with the presence of Mg phases in the bentonite and the existence of C-A-S-H close to the concrete.

To advance this characterization, we applied thermal, infrared and Si and Al NMR methods. The thermal analysis confirms the presence of brucite-like and disordered MSH-like phases with broad dehydroxylation effects between 450 and 550 ºC that are not produced in the bentonite outside the altered rim[26, 33]. The broad 550-650 ºC dehydroxylation of Mnt in these samples and the presence of calcite also make it difficult to discard the presence of other Mg hydrated silicates with very similar effects to those of serpentine.

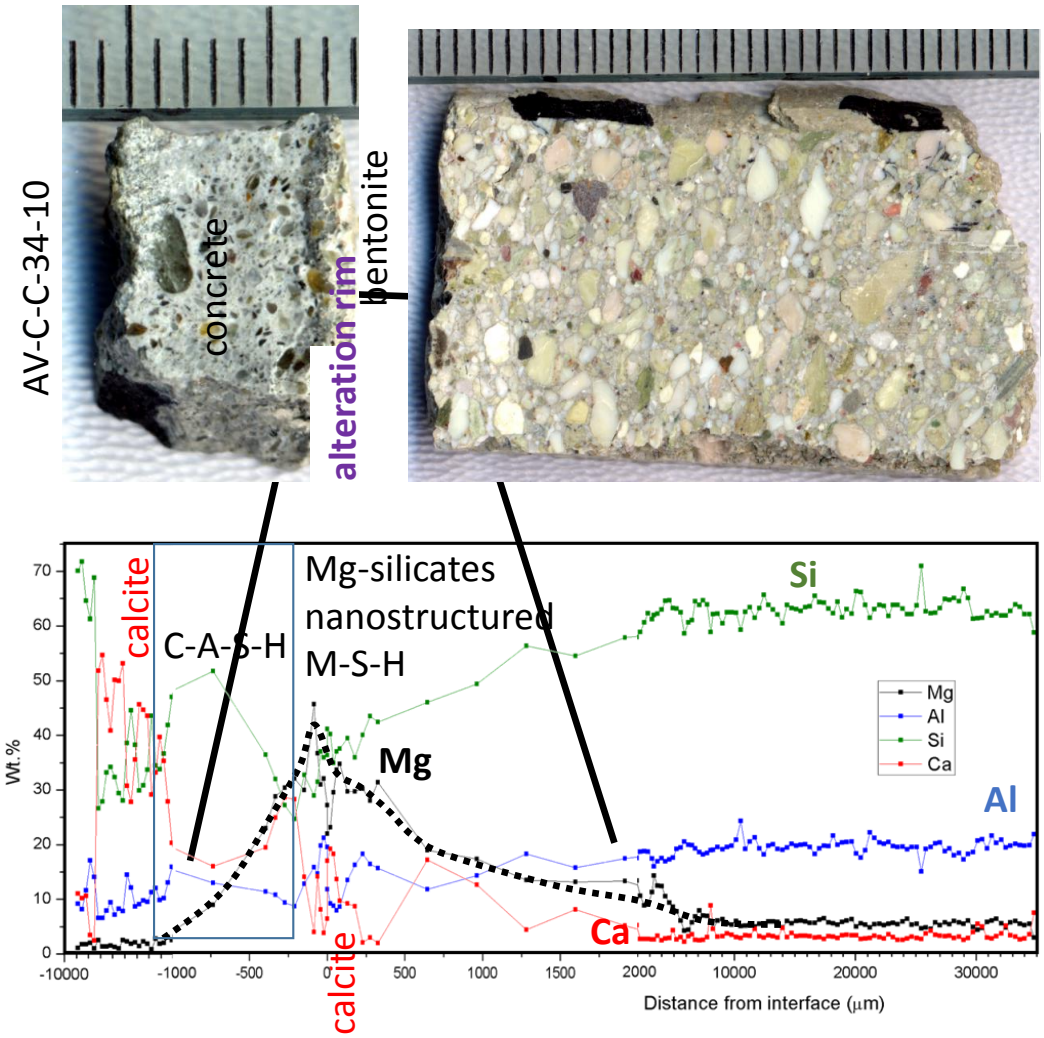

Figure 3. Composition of the chemical analysis and mineralogical zonation (major cations Ca, Si, Al and Mg, excluding C and O and recalculated to 100% (Na, K, Fe, and S not shown)) determined by SEM-EDX showing the characteristic changes in the concrete-FEBEX bentonite interface. Data elaborated from[26]. 0 on the x scale is the contact interface.

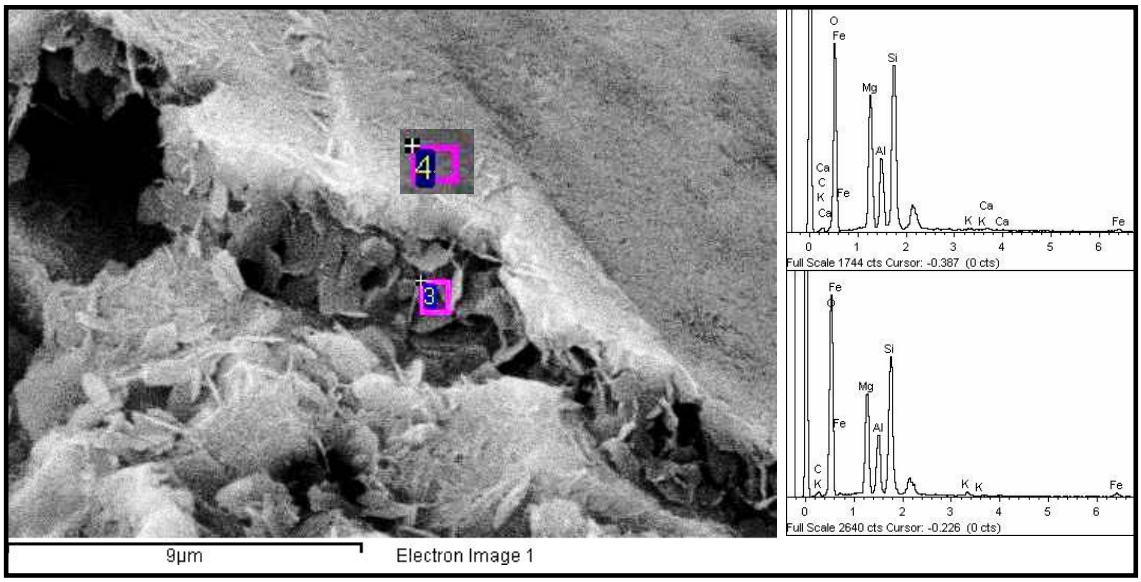

Figure 4: Characteristics of the Mg-rich zone in the alteration rim produced at the contact between concrete and bentonite in a real-scale in situ experiment (FEBEX experiment).

FEBEX- mont $Ca_{0.25}Al_{1.5}Mg_{0.50}Si_4O_{10}(OH)_2$ **Mg/Si: 0.12; Al/Si: 0.38**
FEBEX–brucite $Mg_3(OH)_{5.5}Al_{1.50}Mg_{0.50}Si_4O_{10}(OH)_2$ **Mg/Si: 0.87; Al/Si: 0.38**
Tri-Sme: $Ca_{0.125}Mg_{2.75}Si_4O_{10}(OH)_2$ **Mg/Si: 0.69**
Serpentine: $Mg_3Si_2O_5(OH)_4$ **Mg/Si: 1.50**

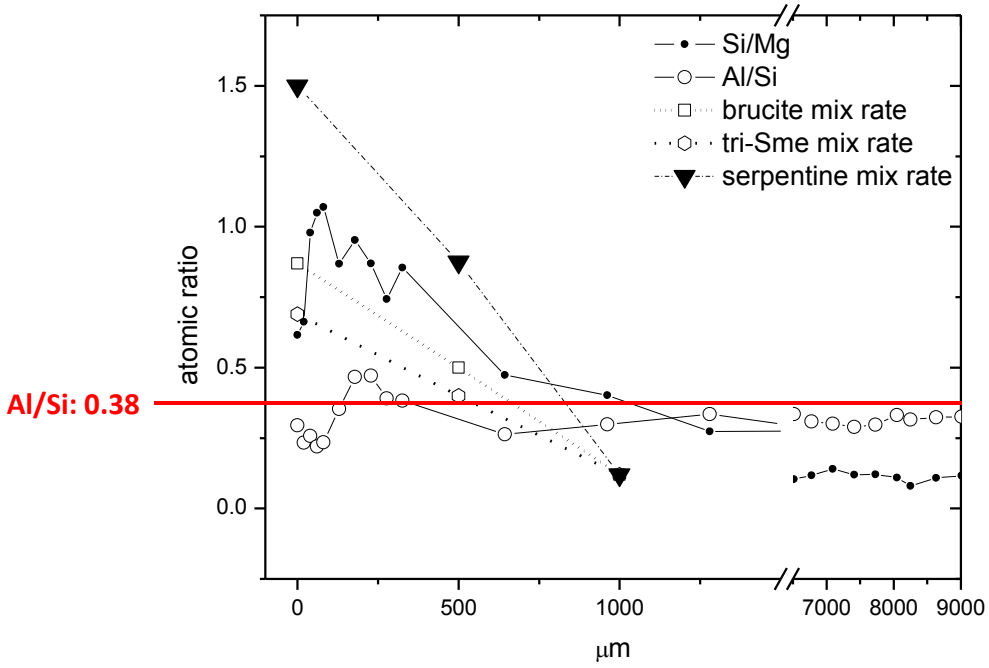

Figure 5: Al/Si and Mg/Si atomic (mol) ratios from the bentonite towards the interface (x=0) with concrete in one of the FEBEX in situ analyzed interfaces. The mix rate trends of different Mg phases and Mnt were calculated (0: 0%; 500: 50% and 1000: 100%).

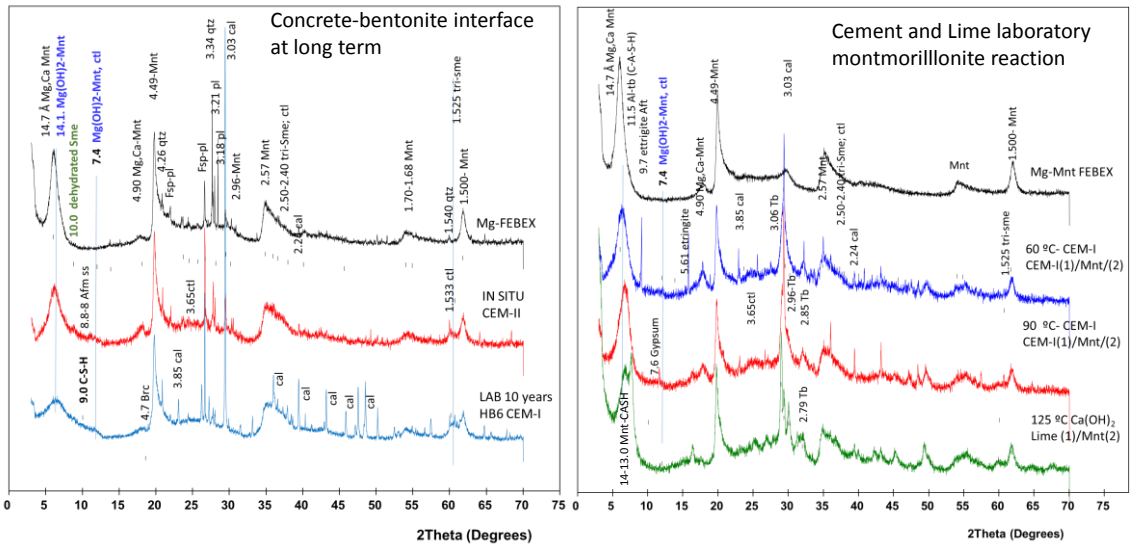

Figure 6. XRD powder patterns comparing the characteristics of the laboratory reactions with lime or cement mixtures and Mnt (right) with long-term concrete-bentonite interfaces. Numbers are in Å. Mnt: montmorillonite, Afm: monosulfate calcium aluminate, ctl: chrysotile, cal: calcite, Tb: tobermorite, Pl: plagioclase, qtz: quartz, Tri-Sm: trioctahedral smectite, Brc: brucite.

The FT-IR spectra of FEBEX montmorillonite (Figure 6) are characterized by the presence of a broad band at approximately 3430 cm^{-1}, corresponding to the water-stretching vibrations, and a shoulder near 3330 cm^{-1} due to an overtone of the bending vibration of water observed at 1640 cm^{-1}. The most intense band near 1040 cm^{-1} is attributed to the Si–O stretching vibrations (in plane), and the Si–O stretching vibrations (out of plane) are located at approximately 1115 cm^{-1}. The absorption band at 3625 cm^{-1} corresponds to the stretching vibrations of the structural OH groups of montmorillonite, which is typical for smectites with Al in the octahedral sheet. The bands corresponding to the Al–Al–OH and Al–Mg–OH bending vibrations are observed at 910 and 834 cm^{-1}, respectively[34]. Moreover, the bands at approximately 580 and 650 cm^{-1} also presumably involve the Mg-O-H vibrations observed in the spectra of trioctahedral clays[35]. The band at 580 cm^{-1} became more intense in this region for the in situ sample. In addition, three carbonate-related absorption bands were observed at 1430, 875 and 713 cm^{-1}. This sample also presents an additional single absorption in the OH-stretching region at approximately 3705 cm^{-1}, which indicates the presence of Mg-rich phases. Either brucite or trioctahedral smectites (i.e., saponite and stevensite) as well as poorly ordered M-S-H phases[33, 36] exhibited a band centered near 3698 cm^{-1}, corresponding to the characteristic OH vibration of the $Mg(OH)_2$ group. The reaction mixtures with the CEM-I cement paste show additional bands at 1550-1350 cm^{-1}, which can be attributed to CO_3^{2-}. The low absorption intensity of this band is related to the low Ca/Si ratios in the present C-S-H[37].

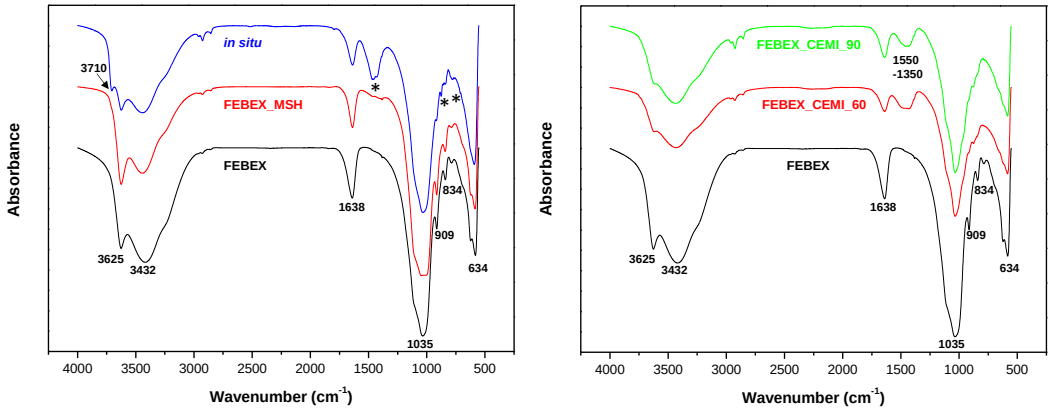

Figure 7: FTIR spectra of FEBEX montmorillonite. Left: comparison with the in situ concrete interface alteration rim and the alkali-treated Mg-montmorillonite (FEBEX MSH); right: comparison of FEBEEX montmorillonite with the reaction mixtures with the CEM-I cement paste.

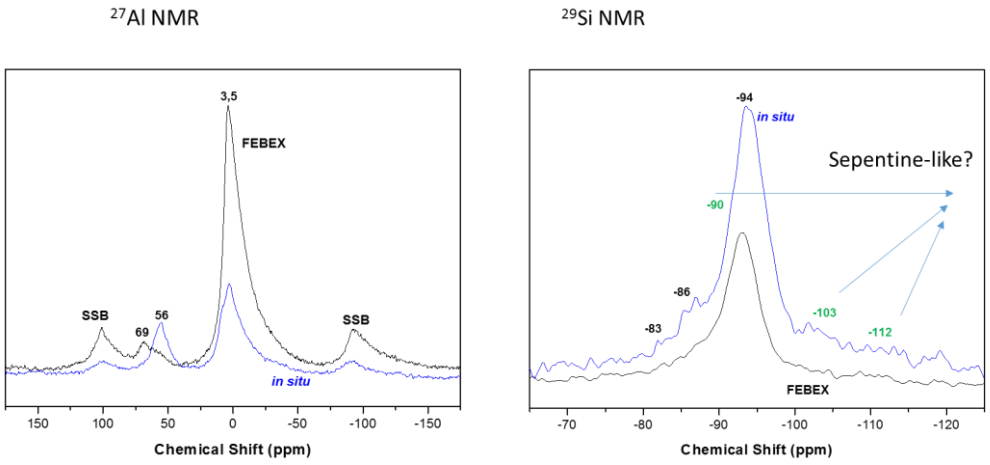

In situ FEBEX

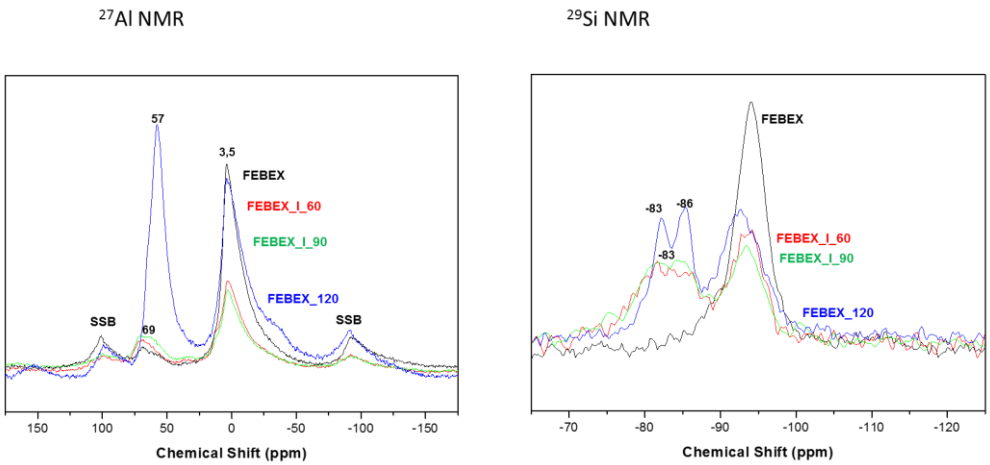

Laborary batch reactions
FebeX Mnt + CEM-I

Figure 8: ^{29}Si and ^{27}Al MAS NMR spectra of the FEBEX samples taken from the concrete interface in the in situ experiment (above) and produced during the reaction of FEBEX montmorillonite with cement paste CEM I(I) at 60 -90 ºC or lime $Ca(OH)_2$ at 120 ºC (below). SSB denotes spinning side bands.

The ^{27}Al MAS NMR spectra clearly show resonances in the region 70-55 ppm and at approximately 2.5 ppm, which correspond to aluminum atoms in tetrahedral and octahedral coordination, respectively[38]. The dominant resonance in FEBEX montmorillonite corresponds to the octahedral environment of Al, and the two poorly resolved peaks at approximately 56 and 69 ppm can be attributed to the four-coordinated tetrahedral Al core [39], but the different chemical shifts suggest a different local structure, i.e., a small Al substitution in the tetrahedral sheet with the calculated structural formula $K_{0.04\pm0.01}Ca_{0.24\pm0.06}(Fe_{0.09}\ Al_{1.41}\ Mg_{0.50})Si_{3.94}\ Al_{0.05}(O_{10}\ (OH)_2)$[15], and the presence of minor feldspar impurities. In both the in situ samples and batch cement paste reactions, the four-coordinated tetrahedral Al resonance increases to represent a comparable amount of octahedral Al. This cannot be attributed to feldspar impurities and

confirms the presence of C-A-S-H phases. The presence of a $–OAl(OSi)_3$ site in the C–S–H structure also implies the presence of a Q3 (1Al) ^{29}Si site [40].

Regarding the ^{29}Si MAS NMR spectra of montmorillonite, the dominant resonance appears at approximately -93 ppm and is present in all the spectra (Figure 7), and this resonance corresponds to the $Si0_4$ groups in the tetrahedral sheet of montmorillonite that are connected to the zero tetrahedron in which Al substitutes for Si, i.e., Q3(0Al) units. However, in the cement paste or lime reacted montmorillonite (60-90-120 ºC) and in the in situ experiments, the contribution from the Q3(0Al) resonance decreases, and new resonances appear between -82 and -86 ppm, which can be related to several types of connectivity between the aluminum-silicate groups and the CSH and CASH phases[23]. The chemical shift of ^{29}Si at ∼–86 ppm is assigned to tetrahedral Si, which is bonded in the middle of silicate chains (Q2). When aluminum was incorporated into the silicate chain as a bridging tetrahedron, an additional peak was observed at approximately –83 to -81 ppm (Q2 [1Al]; [41, 42].

The presence of C-A-S-H nanophases at the concrete-bentonite interfaces has been confirmed by NMR methods, and they are characteristic reactivity products of cementitious material and bentonite. Unfortunately, the exact nature of the Mg-silicate phase was not determined despite the thermal, IR and XRD data confirming the existence of Mg hydroxylated phases.

Concept of the concrete-bentonite interface as a new physical-chemical barrier for safety protection

The complex mixture of disordered mineral compounds characteristic of the alteration rim produced in one of the EBS interfaces proposed for a nuclear DGR repository has been shown. During cement degradation, several pH buffered stages develop, ensuring the longevity of cement. Similarly, the microstructure of the reacted concrete-bentonite interface can be considered a self-built mineral zone region that is useful for buffering subsequent mineral reactions. The capacity of several materials to buffer and stabilize the pH will be important for this concept. During the laboratory batch reactions using the CEM-I paste, we measured the pH evolution. For the alkali-treated Mg-montmorillonite ($Mg(OH)_2$ precipitate with montmorillonite), we added calcite to the obtained products, and we measured the pH evolution. These two materials mimic C-A-S-H (and calcite) and Mg-hydroxide-silicate (and calcite). Mg-saturated, untreated bentonites were also equilibrated with calcite, which represented the bulk bentonite buffer material. The pH evolution is presented in Figure 9. The pH quickly stabilized in the explored systems, which is not common in experiments with colloidal mineral materials. The pH values were consistent with the reported pH range during C-A-S-H formation[43] and brucite precipitation[44].

Despite the need to explain the multiple equilibrium reactions that control this complex system, including the surface reactions, a correlation exists between the measured, stabilized pH values and the mineral zones that are described to form in the concrete-bentonite interface. Radionuclides commonly behave as heavy metal ions. Some of them behave as simple cations, such as Cs^+, $Ni^{2+,}$ and Sr^{2+}, and they can be retained in the near-neutral bentonite region [45]. Komarneni and coworkers[46] studied the sorption of cations (Pb^{2+}, Cd^{2+}, Mn^{2+}, Zn^{2+}, Cu^{2+}, Mg^{2+}, Co^{2+}, or Ni^{2+}) on crystalline C-S-H (tobermorite) in aqueous systems and found Ca^{2+} in the C-S-H was replaced by the cations. Thus, these cations can also be retained in the aged concrete regions near the bentonite. Oxy cations such as PuO_2^{2+} or NpO^{2+} can also be retained in bentonite. They form stable complexes with inorganic carbon species, and they can be

transported as ion pairs or anions[47]. These species become depleted as the pH rises (calcite precipitation), and they can be retained or adsorbed near the M-S-H region[48, 49]. Stable oxyanions, such as SeO_3^{2-}, SeO_4^{2-}, TcO_4^-, MoO_4^{2-} or CrO_4^-, can be retained by the C-(A)-S-H or Afm or Aft solid solutions in which OH^- and CO_3^{2-} anions can also integrate with the major anions characterizing such structures[50, 51]. These RNs are expected to be retained in the C-A-S-H degraded zone of concrete. There is some scientific debate about the capacity of C-S-H-like phases to retain metals, oxyanions and anions. A recent paper[52] concluded that chloride, bromides and nitrates do not specifically adsorb on C-S-H particles, but they tend to accumulate in a diffuse layer where they compete with OH^-.

In summary, our goal is to study the geochemically zoned rim in the concrete-bentonite interface as a multi-functional, nanostructured space barrier for radionuclide cations and anions. There are some uncertainties regarding anion retention. Nevertheless, it will be important to know how this barrier will perform as a whole.

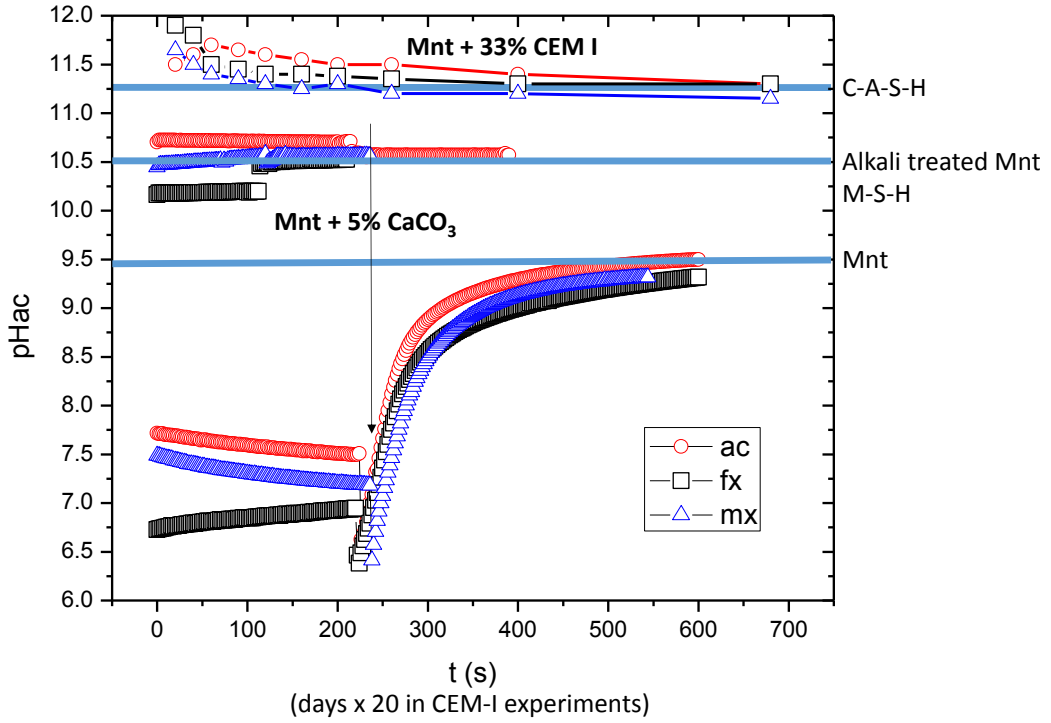

Figure 9. The pH evolution of the different reaction systems, including calcite and montmorillonite. Upper plots: Mnt reacts with the CEM-I cement paste (C-A-S-H formation). Lower plots: pH evolution after calcite addition in suspensions of alkali-treated, Mg-saturated montmorillonite (final pH 10.5) and Mnt (final pH 9.5). See Table 1. ac, fx(febex) and mx are the three bentonites used in the experiments.[27]

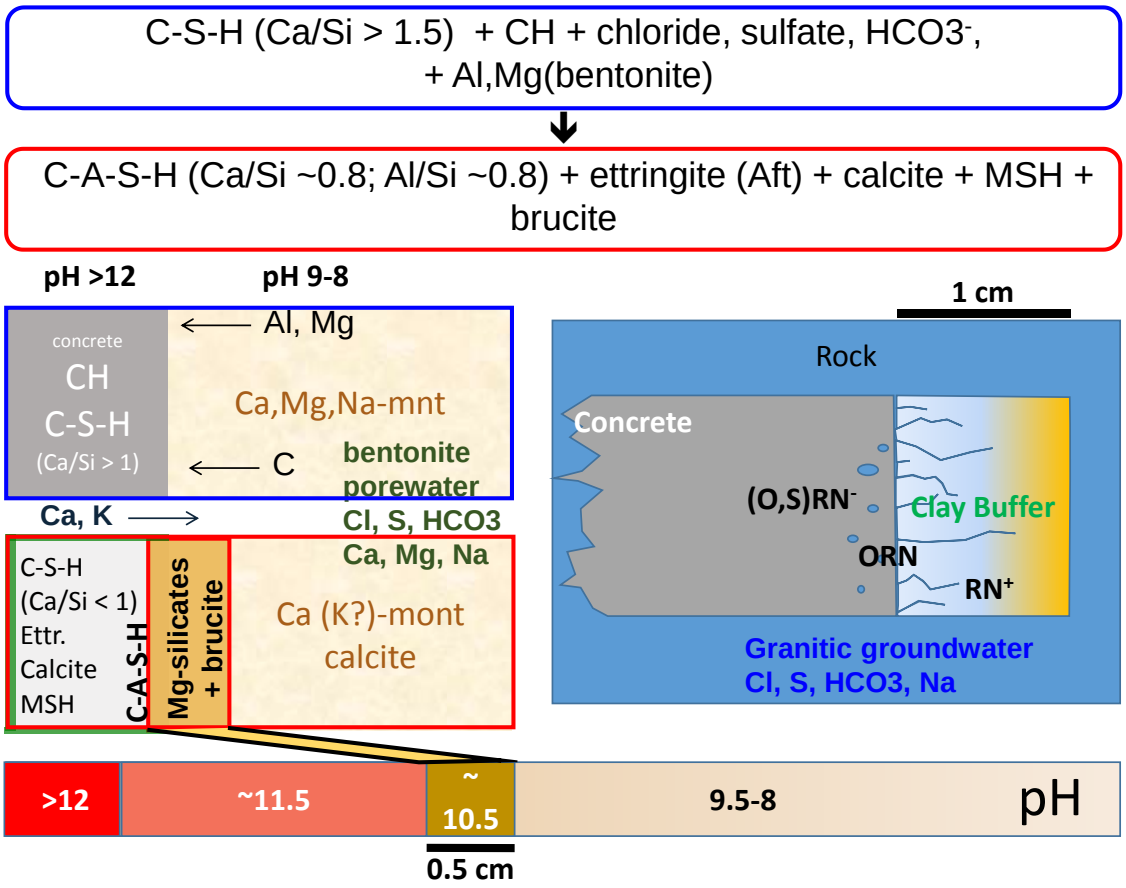

Figure 10: Scheme of the concrete-bentonite reactivity and construction of the zone pH geochemical barrier. CH and C-S-H are $Ca(OH)_2$ and calcium silicate hydrates. Brucite: $Mg(OH)_2$, ettringite is tri-sulfate calcium aluminate ($Ca_6[Al(OH)_6{\cdot}12H_2O]_2$ $(SO_4)_3{\cdot}2H_2O$). Aft is the name of solid solutions of alumina, ferric oxide, and tri-sulfate in which ettringite is the most common. Calcite: CaCO3, (O,S)RN-, ORN and RN+: oxyanions of radionuclide-substituted and Aft phases as precipitated hydroxides or retained as cations. MSH: hydrated magnesium silicates including poorly ordered phases in concrete and nanosize silicate sheets in contact with bentonite. The clay buffer is bentonite.

Acknowledgements

We want to dedicate this paper to professor Santiago Leguey. He started our team to develop and instigate research on the role of Spanish bentonite for nuclear waste isolation in geological environments. He is also a very good science colleague of professor Eduardo Ruiz Hitzky, and we are sure Eduardo would be happy to share some credit with him.

References

1 F. Ridi, E. Fratini, P. Baglioni, *J Colloid Interface Sci* **2011**, *357*, 255-64 10.1016/j.jcis.2011.02.026.

2 D. D. Eberl, *Philosophical Transactions od the Royal Society of London* **1984**, *A 311*, 241-257.

3 B. L. Ehlmann, J. F. Mustard, S. L. Murchie, J. P. Bibring, A. Meunier, A. A. Fraeman, Y. Langevin, *Nature* **2011**, *479*, 53-60 10.1038/nature10582.

4 J. W. Bullard, H. M. Jennings, R. A. Livingston, A. Nonat, G. W. Scherer, J. S. Schweitzer, K. L. Scrivener, J. J. Thomas, *Cement and Concrete Research* **2011**, *41*, 1208-1223 10.1016/j.cemconres.2010.09.011.

5 F. P. Glasser, T. Matschei, *INTERNATIONAL CONGRESS ON THE CHEMISTRY OF CEMENT -CD-ROM EDITION* **2007**, *TH3-13.4*, 14pp.

6 M. Schindler, D. M. Singer, *Elements* **2017**, *13*, 159-164 10.2113/gselements.13.3.159.

7 J. Cuevas, R. V. d. l. Villa, S. Ramírez, L. Sánchez, R. Fernández, S. Leguey, *Journal of Iberian Geology* **2006**, *32*, 147-169.

8 J. Cuevas, J. Samper, M. J. Turrero, K. Wieczorek, in *Book Impact of the Geochemical Evolution of Bentonite Barriers on Repository*

Safety Functions - PEBS Case 4, ed., ed. by Editor, BGR, City, **2014**, Chap. Chapter, pp. 35-42.

9 W. P. Gates, A. Bouazza, G. J. Churchman, *Elements* **2009**, *5*, 105-110 10.2113/gselements.5.2.105.

10 N. Guven, *Elements* **2009**, *5*, 89-92 10.2113/gselements.5.2.89.

11 F. Huertas, B. d. l. Cruz, J. L. Fuentes-Cantillana, E. Alonso, J. Linares, J. Samper, F. Elorza, C. Svemar, J.-P. Salo, A. Muurinen, J. Pacovský, J. Verstricht, B. Bazargan-Sabet, N. Jockwer, B. Vignal, H. Shao, W. Kickmaier, B. Baeyens, L. Börgesson, I. Rhén, F. Villieras, J. C. Robinet, J. C. Gourry, in *Book Full-Scale Engineered Barriers Experiment for a Deep Geological Repository for High-Level Waste in Crystalline Host Rock – Phase II FEBEX II*, ed., ed. by Editor, City, **2005**, Vol. EUR 21922, Chap. Chapter, pp. 52pp.

12 J. Cuevas, R. Fernández, A. I. Ruiz, A. Ortega, J. González-Yélamos, D. González-Santamaría, in *Book Definition of sampling and characterization of in-situ FEBEX-OPC concrete contact and design of new experiments studying surface interface reactivity*, ed., ed. by Editor, Karlsruher Institut für Technologie (KIT)

KIT Scientific Publishing, City, **2016**, Chap. Chapter, pp. 120-129.

13 U. S. DOE, **2014**, *Volume I. Prepared for U.S. Department of Energy Used Fuel Disposition Campaign by Sandia National Laboratories.*155pp.

14 K. D. Cowley, *Physics Today* **1997**, *50*, 32-39.

15 J. Cuevas, A. I. Ruiz, R. Fernández, in *Book Comparison of alternative bentonites for potential use as buffer and sealing materials in the Swiss concept for radioactive waste disposal. Part 1: Methodology*, ed., ed. by Editor, City, **2013**, Vol. NAB 13-69, Chap. Chapter, pp. 69pp.

16 N. R. Smart, B. Reddy, A. P. Rance, D. J. Nixon, N. Diomidis, *Corrosion Engineering, Science and Technology* **2017**, *52*, 113-126 10.1080/1478422x.2017.1316088.

17 F. P. Glasser, in *Book The Behaviours of Cementitious Materials in Long Term Storage and Disposal of Radioactive Waste*, ed., ed. by Editor, City, **2013**, Vol. 44, Chap. Chapter.

18 D. Savage, in *Book An Assessment of the Impact of the Long Term Evolution of Engineered Structures on the Safety-Relevant Functions of the Bentonite Buffer in a HLW Repository*, ed., ed. by Editor, City, **2014**, Vol. 13-02, Chap. Chapter, pp. 88pp.

19 R. Fernández, M. Rodríguez, R. V. d. l. Villa, J. Cuevas, *Geochimica et Cosmochimica Acta* **2010**, *74*, 890-906 10.1016/j.gca.2009.10.042.

20 A. MEUNIER, B. VELDE, L. GRIFFAULT, *Clay Minerals* **1998**, *33*, 187-196.

21 S. Aggarwal, M. J. Angus, A. Tyson, *Waste Management* **1990**, *2*, 399-406.
22 R. Fernández, L. González, A. I. Ruiz, J. Cuevas, *Journal of Geochemistry* **2014**, *2014*, 1-8 10.1155/2014/145425.
23 R. Fernández, A. Isabel Ruiz, J. Cuevas, *Clay Minerals* **2016**, *51*, 223-235 10.1180/claymin.2016.051.2.09.
24 J. Cuevas, M. Angulo, D. González-Santamaría, J. González-Yélamos, R. Fernández, A. Ortega, A. I. Ruiz, Second Annual Workshop of the HORIZON 2020 CEBAMA Project, Barcelona Spain, **2017**.
25 M. C. Alonso, J. L. García Calvo, J. Cuevas, M. J. Turrero, R. Fernández, E. Torres, A. I. Ruiz, *Physics and Chemistry of the Earth, Parts A/B/C* **2017**, *99*, 38-48 10.1016/j.pce.2017.03.008.
26 R. Fernández, E. Torres, A. I. Ruiz, J. Cuevas, M. C. Alonso, J. L. García Calvo, E. Rodríguez, M. J. Turrero, *Physics and Chemistry of the Earth, Parts A/B/C* **2017**, *99*, 49-63 10.1016/j.pce.2017.01.009.
27 R. Fernández, A. I. Ruiz, J. Cuevas, *Applied Clay Science* **2014**, *95*, 83-94 10.1016/j.clay.2014.03.015.
28 J. Cuevas, A. I. Ruiz, R. Fernández, E. Torres, A. Escribano, M. Regadío, M. J. Turrero, *Applied Clay Science* **2016**, *124-125*, 79-93 10.1016/j.clay.2016.01.043.
29 R. Fernández, R. Vigil de la Villa, A. I. Ruiz, R. García, J. Cuevas, *Applied Clay Science* **2013**, *83-84*, 357-367 10.1016/j.clay.2013.07.021.
30 I. G. Richardson, *Cement and Concrete Research* **2008**, *38*, 137-158 10.1016/j.cemconres.2007.11.005.
31 I. G. Richardson, *Acta Crystallogr B Struct Sci Cryst Eng Mater* **2014**, *70*, 903-23 10.1107/S2052520614021982.
32 C. Roosz, S. Grangeon, P. Blanc, V. Montouillout, B. Lothenbach, P. Henocq, E. Giffaut, P. Vieillard, S. Gaboreau, *Cement and Concrete Research* **2015**, *73*, 228-237 10.1016/j.cemconres.2015.03.014.
33 D. Nied, K. Enemark-Rasmussen, E. L'Hopital, J. Skibsted, B. Lothenbach, *Cement and Concrete Research* **2016**, *79*, 323-332 10.1016/j.cemconres.2015.10.003.
34 J. Madejova, M. Pentrak, H. Palkova, P. Komadel, *Vibrational Spectroscopy* **2009**, *49*, 211-218.
35 P. A. Schroeder, CMS Workshop Lecture, **2002**.
36 J. L. M. D. Vidales, M. Pozo, J. M. Alia, F. Garcia-Navarro, F. Rull, *Clay Minerals* **1991**, *26*, 329-342.
37 S. Grangeon, F. Claret, C. Roosz, T. Sato, S. Gaboreau, Y. Linard, *J Appl Crystallogr* **2016**, *49*, 771-783 10.1107/S1600576716003885.
38 A. D. Irwin, J. S. Holmgren, J. Jonas, *J. Mater. Sci.* **1988**, *23*, 2908-2912.
39 X. Pardal, F. Brunet, T. Charpentier, I. Pochard, A. Nonat, *Inorg Chem* **2012**, *51*, 1827-36 10.1021/ic202124x.
40 T. F. Sevelsted, J. Skibsted, *Cement and Concrete Research* **2015**, *71*, 56-65 10.1016/j.cemconres.2015.01.019.
41 I. G. Richardson, A. R. Brough, R. Brydson, G. W. Groves, C. M. Dobson, *Journal of the American Ceramic Society* **1993**, *76*, 2285-2288
42 G. K. Sun, J. F. Young, R. J. Kirkpatrick, *Cement and Concrete Research* **2006**, *36*, 18-29 10.1016/j.cemconres.2005.03.002.
43 I. Garcia-Lodeiro, A. Palomo, A. Fernández-Jiménez, D. E. Macphee, *Cement and Concrete Research* **2011**, *41*, 923-931 10.1016/j.cemconres.2011.05.006.
44 O. S. Pokrovsky, J. Schott, *Geochimica et Cosmochimica Acta* **2004**, *68*, 31-45 10.1016/s0016-7037(03)00238-2.

45 D. G. Brookins, *Geochemical aspects of radioactive waste disposal*. Editor, Spriger-Verlag New YorK, **1984**.
46 S. Komarneni, E. Breval, D. M. Roy, R. Roy, *Cement and Concrete Research* **1988**, *18*, 204-220.
47 S. Salah, L. Wang, in *Book Speciation and solubility calculations for waste relevant radionuclides in Boom Clay*, ed., ed. by Editor, City, **2014**, Vol. EXTERNAL REPORT SCK•CEN-ER-198, Chap. Chapter, pp. 154pp.
48 T. Zhang, C. R. Cheeseman, L. J. Vandeperre, *Cement and Concrete Research* **2011**, *41*, 439-442 10.1016/j.cemconres.2011.01.016.
49 M. Tonelli, F. Martini, L. Calucci, E. Fratini, M. Geppi, F. Ridi, S. Borsacchi, P. Baglioni, *Dalton Trans* **2016**, *45*, 3294-304 10.1039/c5dt03545g.
50 S. M. Leisinger, B. Lothenbach, G. L. Saout, R. Kägi, B. Wehrli, C. A. Johnson, *Environ. Sci. Technol.* **2010**, *44*, 8983–8988
51 V. A. Drebushchak, Y. V. Seryotkin, S. N. Kokh, E. V. Sokol, *Journal of Thermal Analysis and Calorimetry* **2013**, *114*, 777-783 10.1007/s10973-013-2989-3.
52 G. Plusquellet, A. Nonat, *Cement and Concrete Research* **2016**, *90*, 89-96.